Numerical investigation of the enhanced unidirectional surface plasmon polaritons generator*

Zhang Zhi-Dong(张志东)[a], Wang Hong-Yan(王红艳)[a]†, Zhang Zhong-Yue(张中月)[b], and Wang Hui(王 辉)[a]

[a] School of Physical Science and Technology, Southwest Jiaotong University, Chengdu 610031, China
[b] School of Physics and Information Technology, Shaanxi Normal University, Xi'an 710062, China

(Received 7 April 2013; revised manuscript received 26 June 2013; published 12 November 2013)

A unidirectional surface plasmon polaritons (SPPs) generator with greatly enhanced generation efficiency is proposed. The SPPs generator consists of an asymmetric single nanoslit coated with a polyviny alcohol (PVA) film and a silver rectangle block. The generation efficiency of this SPPs generator is investigated using the finite difference time domain method. Due to the presence of the silver rectangle block, the SPPs generation efficiency of the asymmetric single nanoslit with PVA film can be greatly enhanced and the corresponding wavelength with the maximum enhancement factor can be tuned flexibly. The influence of the structural parameters on the generation efficiency is also investigated for the enhanced unidirectional SPPs generator.

Keywords: surface plasmon polariton, surface plasmon polaritons (SPPs) generator, asymmetric single-slit, finite difference time domain method

PACS: 78.68.+m, 73.20.Mf **DOI:** 10.1088/1674-1056/23/1/017801

1. Introduction

Surface plasmon polaritons (SPPs), propagating along the metal–insulator interface with an exponentially decaying electric field on both sides, have great potential as a new generation of information carriers: highly integrated nanophotonic devices.[1–4] Although many ultracompact optical devices based on SPPs have been proposed and demonstrated[5–8], the efficient excitation method of SPPs remains the one fundamental issue in plasmonics. SPPs usually cannot be directly excited by the plane wave light.[9,10]

Some novel SPPs generators composed of subwavelength metal structures with symmetrical slits were proposed in Refs. [11]–[13]. Due to the spatial symmetry of these structures, the SPPs were excited and propagated equivalently in opposite directions along the interface between the metal and insulator. These SPPs generators not only decrease the generation efficiency but also restrict their applications, especially when only one SPPs direction is necessary.[14–16] In order to obtain unidirectional SPPs generators, a subwavelength metal single-slit structure with a nanogroove is presented.[16–19] With properly designed structural parameters and back-side illumination, the asymmetric subwavelength single-nanoslit can efficiently generate unidirectional SPPs without the incident light noise.[18,19] The left-going SPPs are mainly contributions by the SPPs interference from the different round trips in the Fabry–Perot (FP) nanocavity. The right-going SPPs are mainly contributions by the interference between the directly excited SPPs and the scattered SPPs from the nanocavity.[18] Recently, Li *et al.*[20] proposed that the subwavelength holes blocked by the metal disk structure can enhance the light transmission through the subwavelength hole. Here, the metal disk behaves as a transmitting antenna, which can enhance the emission efficiency through exciting the localized plasmons.

Considering the generation efficiency and unidirectionality simultaneously, we propose an enhanced unidirectional SPPs generator whose SPPs generation efficiency is dramatically enhanced by introducing a subwavelength silver rectangle block on top of the asymmetric metal single slit. The generation efficiency is investigated by the finite-difference time-domain method (FDTD) and compared with the regular unidirectional SPPs generator without the silver rectangle block. The effects of the structural parameters of the enhanced unidirectional SPPs generator on the generation efficiency are also studied.

2. Enhanced unidirectional SPPs generator structure and computational methods

The schematic diagram of the enhanced unidirectional SPPs generator structure is illustrated in Fig. 1, which is composed of an asymmetric single slit coated with PVA (refractive index $n_{\mathrm{PVA}} = 1.5$) film and a silver rectangular block. When the enhanced unidirectional SPPs generator is illuminated by a *p*-polarized plane wave from the back side, two SPPs are generated and propagated to opposite directions. The metal sur-

*Project supported by the National Natural Science Foundation of China (Grant Nos. 11174237 and 10974161), the National Basic Research Program of China (Grant No. 2013CB328904), the Fundamental Research Funds for the Central Universities of Ministry of Education of China (Grant Nos. SWJTU12CX084 and SWJTU2010ZT06), and the Innovation Fund for Ph. D. Student of Southwest Jiaotong University, China.

†Corresponding author. E-mail: hongyanw@home.swjtu.edu.cn

face obtains better SPPs field confinement when the dielectric film is coated.[21–24] The nanogroove has a fixed width of 800 nm and the slit has a fixed width $w = 200$ nm. The nanogroove depth is h. The PVA film thickness is t. The length of the silver rectangular block is S and the height is fixed at 100 nm. The distance between the left-end of nanogroove and the left-end of the silver rectangular block is l. The thickness of the whole structure is fixed at 400 nm (in z direction). The energy flow is determined by the integral of the Poynting vector over the cross section of the port (1, 2, or 3). The generation efficiency is determined by P_T/P_0. Here, P_0 is the energy flow through port 1 when a plane wave through a 200-nm-width slit surrounded by air, P_T is the energy flow along the interface between the PVA film and silver at a distance of 200 nm from the right-end (port 2) or left-end (port 3). The enhancement factor (EF) of the corresponding resonance modes is defined as EF = $P_{with}/P_{without}$ to describe the enhancement of the SPPs generation efficiency. Here, P_{with} and $P_{without}$ represent the energy flow of the unidirectional SPPs generator with and without the silver rectangular block, respectively.

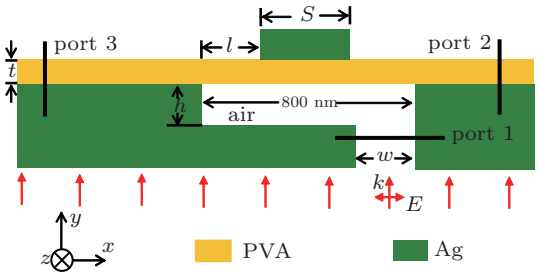

Fig. 1. (color online) Schematic of the enhanced unidirectional SPPs generators.

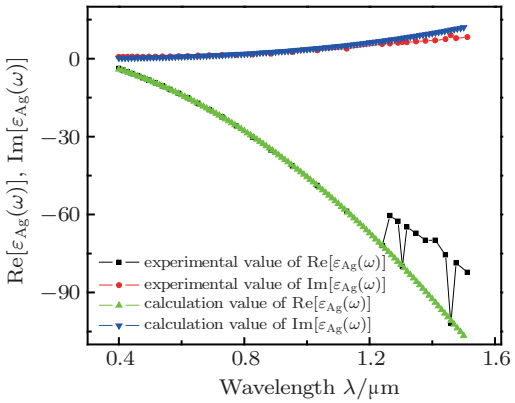

Fig. 2. (color online) Experimental values and calculated values of the silver permittivity.

The generation efficiency of the enhanced unidirectional SPPs generator is simulated by the commercial FDTD software (XFDTD by Remcom Inc.). The frequency-dependent complex relative permittivity $\varepsilon(\omega)$ of silver is characterized by the modified Debye–Drude dispersion model[25]

$$\varepsilon(\omega) = \varepsilon_\infty + \left(\frac{\varepsilon_s - \varepsilon_\infty}{1 + i\omega\tau}\right) + \frac{\sigma}{i\omega\varepsilon_0}.$$

Here, $\varepsilon_s = -9530.5$ represents the static permittivity, $\varepsilon_\infty = 3.8344$ is the infinite frequency permittivity, $\sigma = 1.1486 \times 10^7$ S/m is the conductivity and $\tau = 7.35 \times 10^{-15}$ is the relaxation time. The calculated value using the Debye–Drude model and the experimental value of the silver permittivity are plotted in Fig. 2. The imaginary part of the calculated value agrees well with the experimental value in the chosen wavelength range (0.4 μm–1.5 μm). However, for the real part, the calculated value fits well in the wavelength range of 0.4 μm–1.2 μm, but does not fit well in the wavelength range of 1.2 μm–1.5 μm. Therefore, the simulation results are more reasonable in the wavelength range of 0.4 μm–1.2 μm.

3. Results and discussion

3.1. Generation efficiency and enhancement mechanism

The generation efficiencies as a function of the incident light wavelength for the unidirectional SPPs generator with and without the silver rectangular block enhancement are shown in Fig. 3, in which the structural parameters of the enhanced unidirectional SPPs generator are $S = 400$ nm, $l = 200$ nm, $t = 100$ nm, and $h = 150$ nm. The generation efficiencies of the right-going and left-going SPPs without the silver rectangular block are represented by the black line and red line in Fig. 3, respectively. The green line and blue line denote the counterparts for the enhanced case with the silver rectangular block. The generation efficiencies curve of the right-going SPPs in the regular unidirectional SPPs generator and the enhanced unidirectional SPPs generator show similar resonant behaviors, in which three peaks are observed. However, the resonant peaks of the enhanced unidirectional SPPs generator are found to red shift relative to the regular unidirectional SPPs generator. For the left-going SPPs, similar resonant behaviors are observed, i.e., three peaks are found for the regular and the enhanced unidirectional SPPs generators and those resonant peaks also red shift for the enhanced unidirectional SPPs generator relative to the regular unidirectional SPPs generator.

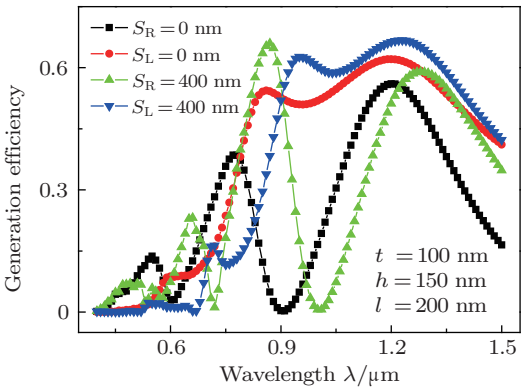

Fig. 3. (color online) Generation efficiency of the left-going and right-going SPPs for the regular unidirectional SPPs generators and the enhanced unidirectional SPPs generators.

The normalized $|H_z|$ field distribution at resonant peaks of the enhanced unidirectional SPPs generators is calculated and compared with the regular unidirectional SPPs generators, which can illustrate the generation efficiencies enhancement mechanism and the resonance-peak red-shift mechanism for the enhanced unidirectional SPPs generator. Figure 4 shows that initial SPPs propagate along the interface between PVA film and silver film to the right and the other SPPs propagate along the bottom of the nanogroove to the left. The upper part of the nanogroove acts as a FP nanocavity. The left-going SPPs are reflected back and forth between the upper two walls of the nanogroove. Thus, the standing waves arise in the nanogroove.

For the regular unidirectional SPPs generator, their mode numbers are 3 at $\lambda = 0.547$ μm and $\lambda = 0.591$ μm. The generated SPPs primarily propagate to the nanoslit right side at $\lambda = 0.547$ μm while primarily they propagate to the left side at $\lambda = 0.591$ μm. At $\lambda = 0.773$ μm and $\lambda = 0.856$ μm, the mode numbers are 2. The generated SPPs primarily propagate to the nanoslit's right side at $\lambda = 0.773$ μm and to the left side at $\lambda = 0.856$ μm, respectively. At $\lambda = 1.196$ μm and $\lambda = 1.203$ μm, the mode numbers are 1. The generated SPPs equally propagate in the opposite directions.

For the enhanced unidirectional SPPs generator, the normalized $|H_z|$ field distribution at $\lambda = 0.654$ μm (as shown in Fig. 4(g)) is different from the regular unidirectional SPPs generator (Fig. 4(a)) because the nanogroove's inherent mode is broken by the silver rectangular block. However, SPPs still primarily propagate to the nanoslit's right side; the corresponding enhancement factor is EF = 1.7. At $\lambda = 0.718$ μm (as shown in Fig. 4(h)), the mode numbers is 3, similar to the regular unidirectional SPPs generator's distribution in Fig. 4(b). The vertical FP-cavity formed by the silver rectangular block and the bottom silver film enhances the SPPs field confinement. The increasing wave vector results in the resonant peak red shift. The corresponding enhancement factor is EF = 1.9, because the vertical FP-cavity enhances the silver rectangular block's transmitting antenna effect, which can enhance the silver rectangular block's emission efficiency through exciting the localized plasmons.[20] The generation efficiency enhancement mechanism and the resonance peaks shift mechanism for the other four resonance peaks ($\lambda = 0.866$ μm, 0.944 μm, 1.220 μm, and 1.278 μm) are the same as when the resonant peak is at $\lambda = 0.718$ μm. At $\lambda = 0.866$ μm and $\lambda = 0.944$ μm (as shown in Figs. 4(i) and 4(j)), the mode distribution is similar to Figs. 4(c) and 4(d) and their mode numbers are 2. The corresponding enhancement factors are 1.7 and 1.2. At $\lambda = 1.278$ μm and $\lambda = 1.220$ μm (as shown in Figs. 4(k) and 4(l)), the mode distribution is similar to that in Figs. 4(e) and 4(f) and their mode numbers are 1. The corresponding enhancement factors are 1.0. The unidirectivity of SPPs can be tuned through adjusting the structural parameters of the lateral nanocavity (the nanogroove).

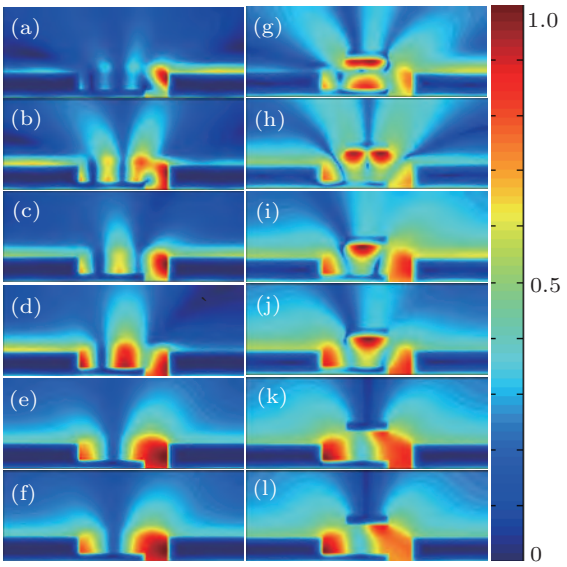

Fig. 4. (color online) Contour profiles of the normalized $|H_z|$ fields of the regular unidirectional SPPs generators: (g) $\lambda = 0.654$ μm, (h) $\lambda = 0.718$ μm, (i) $\lambda = 0.866$ μm, (j) $\lambda = 0.944$ μm, (k) $\lambda = 1.278$ μm, (l) $\lambda = 1.220$ μm and the enhanced unidirectional SPPs generators: (a) $\lambda = 0.574$ μm, bh) $\lambda = 0.591$ μm, (c) $\lambda = 0.773$ μm, (d) $\lambda = 0.856$ μm, (e) $\lambda = 1.196$ μm, (f) $\lambda = 1.203$ μm.

3.2. Influence of structure parameters

Firstly, the nanogroove depth and the PVA film thickness are fixed at $h = 150$ nm and $t = 100$ nm to investigate the effect of the silver rectangular block length S and position l on the generation efficiency of the enhanced unidirectional SPPs generators. The silver rectangular block length S is increased from 100 nm to 400 nm by every 50 nm while the silver rectangular block position l is fixed ($l = 200$ nm). The generation efficiencies of the right-going SPPs are shown in Fig. 5(a). With the increase of the silver rectangualr block's length S, those resonance peaks red shift because the SPPs field confinement is enhanced in the nanogroove. The generation efficiency of those peaks increase with the increase of the silver rectangular block's length S, due to the silver rectangular block's antenna effect and the electrical field coupling effect between the silver rectangular block and two sides of the nanogroove. The silver rectangular block acts as a transmission antenna to enhance the emission efficiency of the silver rectangular block through exciting the localized plasmons,[20] as the electric field amplitude and the scattering intensity of the transmission antenna are amplified by the localized surface plasmon resonance. The generation efficiencies of the left-going SPPs are shown in Fig. 5(b). With the increase of the silver rectangular block's length S, two resonance peaks in the long wavelength range are separated gradually. This is because of the destructive interfacence between the leaking SPPs from the FP nanocavity and the scattering localized surface plasmons resonance from the transmission antenna.

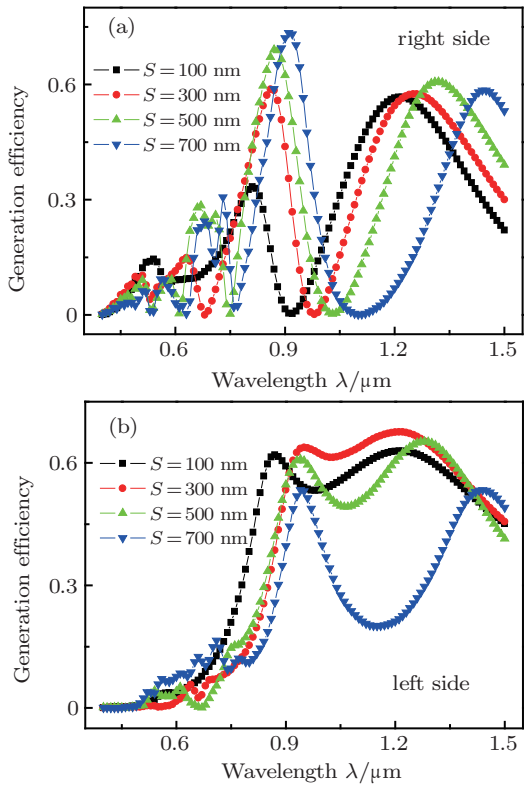

Fig. 5. (color online) Generation efficiency of the enhanced unidirectional SPPs generators with different S: (a) the right-going SPPs, (b) the left-going SPPs.

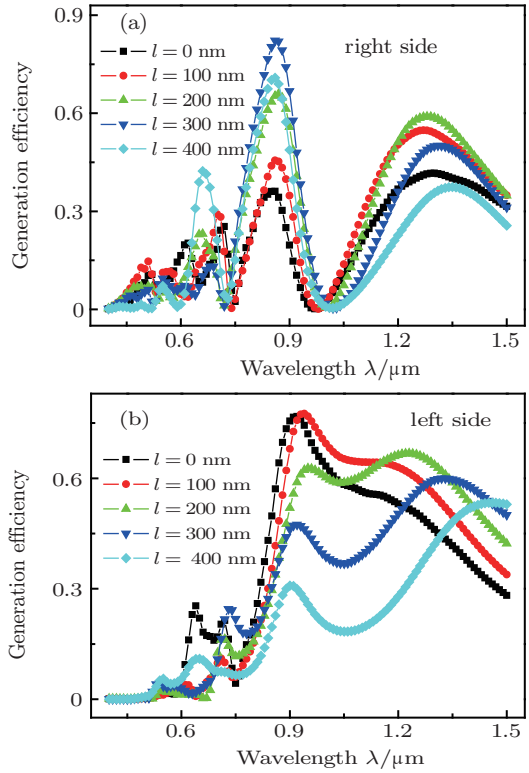

Fig. 6. (color online) Generation efficiency of the enhanced unidirectional SPPs generators with different l: (a) the right-going SPPs, (b) the left-going SPPs.

The effect of the silver rectangular block's position l on the generation efficiency of the enhanced unidirectional SPPs generators is investigated by increasing l from 0 nm to 400 nm with the step size of 50 nm and fixing the silver rectangular block length S at 400 nm. The generation efficiencies of the right-going and left-going SPPs are shown in Figs. 6(a) and 6(b). The generation efficiencies increase with the increase of l, as shown in Fig. 6(a), because the silver rectangular block's right shifts result in the enhancement of the coupling between the nanogroove's right side and the silver rectangular block. For the right-going SPPs generation efficiency, the second resonance peaks (0.86 μm) almost do not shift with the increase of l because the SPPs field confinement is not enhanced by the silver rectangular block shift. For the left-going SPPs generation efficiency, the second peak (0.92 μm) almost does not shift while the generation efficiency decreases apparently with the increase of l, as shown in Fig. 6(b). This is because the position of the resonance peaks are closely related to the length of the silver rectangular block and the length of the FP nanocavity.

The effect of the nanogroove depth h on the generation efficiencies of the enhanced unidirectional SPPs generators is shown in Fig. 7. In this case, the silver rectangular block length S, the distance l between the left-end of the nanogroove and the left-end of the silver rectangular block, and the PVA film thickness t are fixed ($S = 400$ nm, $l = 200$ nm, and $t = 100$ nm). The nanogroove depth h is increased from 90 nm to 230 nm with a step of 20 nm. With the increase of h, three resonance peaks almost do not shift for the right-going SPPs. However, the generation efficiencies increase at the corresponding resonance peaks, as shown in Fig. 7(a), which is because the SPPs FP resonance enhancement leading to SPPs scattering increases from the nanocavity to the nanoslit's right-side.[18] For the left-going SPPs, as shown in Fig. 7(b), the resonance peaks do not red shift with the increase of h. However, the SPPs propagating along the bottom of the nanogroove mainly transmit to the left side when the nanogroove depth becomes small.[18]

The effect of the PVA film thickness t on the generation efficiency of the enhanced unidirectional SPPs generators is investigated by increasing t from 20 nm to 180 nm every 20 nm with fixed structure parameters ($S = 400$ nm, $l = 200$ nm and $h = 150$ nm). Figures 8(a) and 8(b) show that those resonance peaks red shift obviously and the generation efficiencies dramatically increase for the right-going SPPs and left-going SPPs with t increasing. This is because the SPPs are an evanescent field and strongly confined on the metal surface. Therefore, the corresponding wave vector is significantly affected by the thin PVA film.

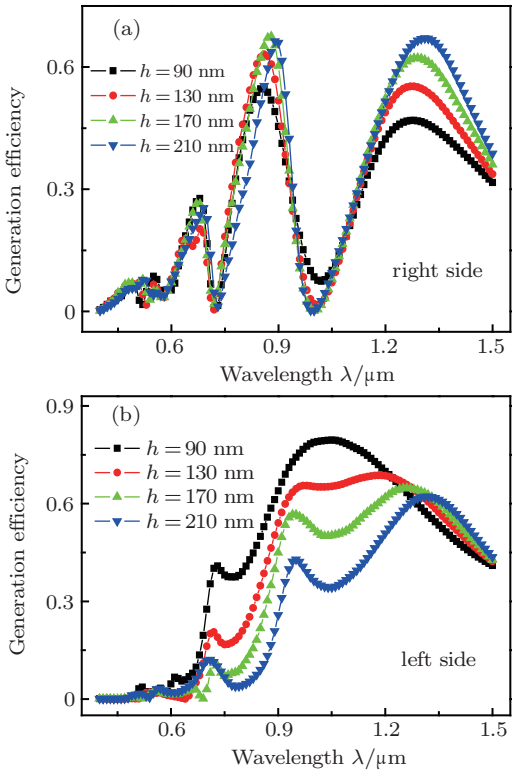

Fig. 7. (color online) Generation efficiency of the enhanced unidirectional SPPs generators with different h: (a) the right-going SPPs, (b) the left-going SPPs.

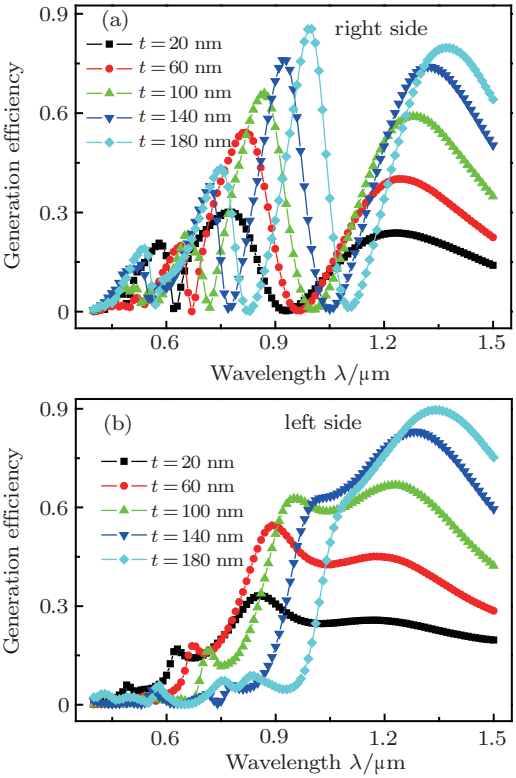

Fig. 8. (color online) Generation efficiency of the enhanced unidirectional SPPs generators with different t: (a) the right-going SPPs, (b) the left-going SPPs.

4. Conclusion

In this paper, an enhanced unidirectional SPPs generator is designed and investigated by the FDTD method. The numerical simulation results show that the generation efficiencies of the enhanced unidirectional SPPs generator are enhanced compared with the regular unidirectional SPPs generator due to the transmitting antennas effects of the silver rectangular block. The resonance-mode red shifts result from the fact that the SPPs field confinement are enhanced by the PVA film and the covered silver rectangular block. The right-going SPPs are mainly contributed by the interference between the directly excited SPPs and the scattered SPPs from the nanocavity. The left-gong SPPs are mainly contributed by the interference of SPPs from the different round trips in the FP nanocavity. The generation efficiency of the enhanced unidirectional SPPs generator strongly depends on the structural parameters. For the silver rectangular block with S = 400 nm and l = 400 nm, the maximal right-going SPPs generation efficiency of the enhanced unidirectional SPPs generator is about three times than that in the regular case. For the silver rectangular block with S = 400 nm and l = 200 nm, the maximal left-going SPPs generation efficiency of the enhanced case maximum is about 1.9 times than that in the regular case. These results provide a novel way to design the unidirectional SPPs generator with higher SPPs generation efficiency.

References

[1] Barnes W L, Dereux A and Ebbesen T W 2003 *Nature* **424** 824
[2] Falk A L, Koppens F H L, Yu C L, Kang K, Snapp N D, Akimov A V, Jo M H, Lukin M D and Park H 2009 *Nat. Phys.* **5** 475
[3] Huang Y, Ye H A, Li S Q and Dou Y F 2013 *Chin. Phys. B* **22** 027301
[4] Yu Z Z, Feng Y J, Wang Z B, Zhao J M and Jiang T 2013 *Chin. Phys. B* **22** 034102
[5] Zhang Z Y, Wang J D, Zhao Y N, Lu D and Xiong Z H 2011 *Plasmonics* **6** 773
[6] Yu Z Z, Feng Y J, Wang Z B, Zhao J M and Jiang T 2013 *Chin. Phys. B* **22** 034102
[7] Lee T W and Gray S K 2005 *Opt. Express* **13** 9652
[8] Zhan C L, Ren X F, Huang Y F, Duan K M and Guo G C 2008 *Chin. Phys. Lett.* **25** 559
[9] Battula A and Chen S C 2006 *Appl. Phys. Lett.* **89** 131113
[10] Groep J, Spinelli P and Polman A 2012 *Nano Lett.* **12** 3138
[11] Li X W, Tan Q F, Bai B F and Jin G F 2011 *Appl. Phys. Lett.* **98** 251109
[12] Xu T, Zhao Y H, Gan D C, Wang C T, Du C L and Luo X G 2008 *Appl. Phys. Lett.* **92** 101501
[13] Li Z, Zhang J S, Yan H F and Gong Q H 2007 *Chin. Phys. Lett.* **24** 3233
[14] Kim H and Lee B 2009 *Plasmonics* **4** 153
[15] Chen J J, Li Z, Yue S, Xiao J H and Gong Q H 2012 *Nano Lett.* **12** 2494
[16] Chen J J, Li Z, Yue S and Gong Q H 2010 *Appl. Phys. Lett.* **97** 041113
[17] Chen J J, Li Z, Yue S and Gong Q H 2011 *J. Appl. Phys.* **109** 073102
[18] Chen J J, Li Z, Lei M, Yue S, Xiao J H and Gong Q H 2011 *Opt. Express* **19** 26463
[19] Chen J J, Li Z, Yue S and Gong Q H 2011 *Nano Lett.* **11** 2933
[20] Li W D, Hu J and Chou S Y 2011 *Opt. Express* **19** 21098
[21] Ebbesen T W, Genet C and Bozhevolnyi S I 2008 *Phys. Today* **61** 44
[22] Chen J J, Li Z and Gong Q H 2009 *Chin. Phys. B* **18** 3535
[23] Verhagen E, Kuipers L K and Polman A 2010 *Nano Lett.* **10** 3665
[24] Gramotnev D K and Bozhevolnyi S I 2010 *Nat. Photonics* **4** 83
[25] Kekatpure R D, Hryciw A C, Barnard E S, Brongersma M L 2007 *Appl. Opt.* **46** 2229
[26] Palik E. D 1985 *Handbook of Optical Constants of Solids* (Florida: Academic Press) p. 355